Title

A modified Cell Transmission Model with realistic queue discharge features at signalized intersections

Authors

Srivastava, Anupam
Jin, Wen-Long
Lebacque, Jean-Patrick

Publication Date

2015-11-01

DOI

10.1016/j.trb.2015.05.013

Peer reviewed

A modified Cell Transmission Model with realistic queue discharge features at signalized intersections

Anupam Srivastava[a], Wen-Long Jin[a,*], Jean-Patrick Lebacque[b]

[a] *Department of Civil and Environmental Engineering, Institute of Transportation Studies, 4000 Anteater Instruction and Research Building, University of California, Irvine, CA 92697-3600*
[b] *Universite Paris-Est, IFSTTAR/COSYS/GRETTIA, F-77447 Champs-sur Marne Cedex, France*

Abstract

Modeling realistic discharge flow-rate and headway features at signalized intersections is critical to the design of traffic signals, since they play a critical role in determining the startup lost times and intersection capacity. Traditional queue discharge models are either microscopic or stochastic, and macroscopic traffic flow models for signalized intersections are based on overly simplistic assumptions. They are incapable of modeling traffic dynamics at signalized intersections as well as capturing realistic queue discharge features.

In this study we propose a modified Cell Transmission Model (CTM) by substituting the traditional demand function, which is constant under over-saturated conditions, with a linearly decreasing function. The new demand function is defined through a combination of conventional macroscopic parameters, including critical density, free-flow speed, jam density, and an additional parameter, jam demand. Analytically we show that the new model reproduces observed features in the discharge flow-rate and headway. We further present a new definition of lost times at the macroscopic level based on the modified CTM. Calibration with observations in existing studies, as well as new observations, further suggest that the model can reasonably capture all traffic queue discharge features. We also discuss solutions to the new model under various Riemann problem scenarios and show that they produce realistic results while offering observable improvements in the modeling of traffic dynamics under certain scenarios.

Keywords: Cell Transmission Model; modified demand function; queue discharge headway and flow-rate; start-up lost time; lost capacity.

*Corresponding author

Email addresses: srivast1@uci.edu (Anupam Srivastava), wjin@uci.edu (Wen-Long Jin), jean-patrick.lebacque@ifsttar.fr (Jean-Patrick Lebacque)

1. Introduction

On a road connecting two signalized intersections, a traffic queue grows when vehicles join it at the upstream queue tail, and dissipates when vehicles leave it from the downstream queue head. The two processes are usually referred to as the queue build-up and discharge processes, respectively. In particular, the queue build-up process occurs when traffic lights at the upstream intersection are green or yellow for some vehicles entering the road, and the queue discharge process occurs when traffic lights at the downstream intersection are green or yellow for vehicles on the road. Therefore the interplay between the two processes determines the formation and dissipation of the traffic queue.

Any complete arterial model of traffic thus needs to model both the queue build-up and discharge processes as well as incorporate network node models, merge-diverge models, and models for any traffic control systems. Queue build-up models typically study the arrival pattern of traffic through the modeling of upstream controls causing vehicles to platoon, and the dispersion of such platoons as they approach the tail of the queue. Platoon dispersion modeling was first studied and modeled in (Pacey, 1956; Robertson, 1969), and has stayed an actively studied field. More recently, various studies such as (Geroliminis and Skabardonis, 2005) have tried to improve on the modeling of the dispersion and thus of travel time of vehicles on links.

Queue discharge features such as the discharge headways and the discharge flow-rate are other critical components to design and analysis of traffic signals at signalized intersections, as they are used to calculate lost times, effective green times, and capacities of different movements. There have been many empirical studies on headway distribution, which can be influenced by the number of lanes, vehicle types, measurement location, and stochasticity (Gerlough and Wagner, 1967; King and Wilkinson, 1977; Kunzman, 1978; Lee and Chen, 1986; Moussavi and Tarawneh, 1990; Niittymäki and Pursula, 1997; Al-Ghamdi, 1999; Hung et al., 2002; Li and Wang, 2006). The earliest queue discharge model developed for traffic at signalized intersections was perhaps in (Webster, 1958), which used existing queue analysis techniques coupled with traffic observations to estimate queue lengths and delays at intersections. Phenomenological models such as (Akçelik and Besley, 2002), and simulation models such as (Tong and Hung, 2002), have been able to correctly predict various queue discharge features. However these models are not easily applied to study traffic dynamics.

Microscopic car-following models have been applied to study the queueing process on a signalized road network and the resulting discharge features (Tian et al., 2002; Bloomberg and Dale, 2000). At the macroscopic level, the Lighthill-Whitham-Richards (LWR) model (Lighthill and Whitham, 1955; Richards, 1956) has been widely applied to calculate the queue length at a signalized intersection and analyze traffic dynamics in a signalized road network, usually without considering lane channelization. For example, the signal control problem is solved based on the LWR model (Michalopoulos et al., 1981); and periodic traffic patterns and corresponding macroscopic fundamental diagram were studied with the network kinematic wave model for a double-ring network in (Jin et al., 2013).

Since (Lighthill and Whitham, 1955), it has been shown with the characteristics method

that, when the downstream traffic light turns green, the discharge flow-rate at the stop-line is always at capacity until the queue disappears. This suggests that the discharge headways at the stop-line are also constant. However, observed headways decrease with the number of vehicles and approach a saturation value with the 5^{th} or 6^{th} vehicle (Greenshields et al., 1946). Further in (Akçelik and Besley, 2002), models for the distributions of both discharge headways and flow-rates were proposed based on observations. In literature, when applying the LWR model to analyze the queueing process at a signalized intersection, one usually assumes that the discharge process only occurs during an ''effective'' green time, not the actual green time (Stephanopoulos et al., 1979). Here the yellow signal and the impact of the dilemma zone are also approximately included in the effective green time. Note that the effective green time is defined at the microscopic level, and is equal to the phase time minus the start-up and clearance lost times (Roess et al., 2010). But it is not clear whether such an approximation is reasonable or not. In summary, the LWR model cannot capture the realistic queue discharge features.

By nature, the unrealistic queue discharge property of the LWR model, in which the discharge flow-rate immediately increases to the capacity when the green period starts, stems from the implicit assumption of an infinite acceleration rate for vehicles leaving an initial standing queue. In literature, some efforts have been made to introduce bounded acceleration to the LWR model on a homogeneous road or at a bottleneck (Lebacque, 1997, 2003; Leclercq, 2002). But these models turn out to be of higher orders and are challenging to analyze, calibrate, and validate.

In this paper, we propose to modify the Cell Transmission Model (CTM) (Daganzo, 1995), which is the Godunov discrete version of the LWR model, to capture queue discharge features after traffic light turns green. We further focus specifically on the through movements and ignore impacts of all turning movements. CTM has been used towards a variety of tasks such as network modeling (Jin et al., 2013), dynamic traffic assignment (Lo, 1999), and urban intersections (Chen et al., 2008). However, the traditional CTM cannot capture the queue discharge features. Here we apply a new demand function, which linearly decreases in density under over-saturated conditions. Since such a modified demand function was first introduced in (Lebacque, 2003), where the bounded nature of acceleration in discharging vehicles was studied within the framework of higher-order kinematic wave models, it is not surprising the modified CTM can replicate realistic discharge headway and flow-rates. One advantage of the presented model is that only one new jam demand parameter is added, and the model can be analyzed and calibrated with minimal efforts.

The rest of the paper is organized as follows. We first review existing models for intersection queue discharge in Section 2. We then present the new demand function and corresponding modified CTM in Section 3. In Section 3.2, we present numerical solutions to the model under the Riemann initial conditions and highlight the difference between the modified CTM and the original CTM in traffic dynamics after the traffic light turns green. In Section 4 we analytically solve the queue discharge headways and flow-rates and present a macroscopic definition of the start-up lost time. In Section 5 we present the calibration

results of the model with field data obtained through various sources and show that the model captures realistic features after being calibrated. We conclude with some closing remarks in Section 6.

2. Review of Cell Transmission Model and its queue discharge features

2.1. Review of CTM

Denoting traffic density k, speed v, and flow-rate q as functions of space and time, we can derive the following LWR model from the flow conservation equation together with the fundamental relationship between density and flow-rate as $q = Q(k)$:

$$\frac{\partial k}{\partial t} + \frac{\partial Q(k)}{\partial x} = 0, \tag{1}$$

which is a hyperbolic conservation law in k. The LWR model can be solved analytically with the characteristics method and numerically with the Godunov method.

In (Daganzo, 1995), a new discrete version of the LWR model, the Cell Transmission Model, was develop by first defining demand (sending flow) and supply (receiving flow) of a cell as a function of traffic density and then calculating boundary fluxes from upstream demands and downstream supplies. Earlier attempts along this line were reported in (Lebacque, 1984, 1993). The conceptual framework of CTM is illustrated in Figure 1: Figure 1a shows the demand and supply curves most commonly used in macroscopic models, corresponding to the triangular fundamental diagram

$$Q(k) \quad = \quad \min\{v_f k, w(k_j - k)\}, \tag{2}$$

where v_f is the free-flow speed, $-w$ the shock wave speed in congested traffic, and k_j the jam density; Figure 1b shows the discretization of a link into cells and the computation of boundary fluxes. That is, in the first step, if we denote traffic density in cell i at a time step by k_i, then the demand and supply are given by

$$D_i \quad = \quad D(k_i) = \min\{v_f k_i, q_c\}, \tag{3}$$

$$S_i \quad = \quad S(k_i) = \min\{q_c, w(k_j - k_i)\}, \tag{4}$$

where $q_c = v_f k_c$ is the capacity or the saturation flow-rate, and $k_c = \frac{v_f w}{v_f + w} k_j$ is the critical density; then in the second step, the boundary flux from cell $i-1$ to cell i is calculated as[1]

$$\Phi_i = \min\{D_{i-1}, S_i\}; \tag{5}$$

[1]Boundary conditions at the upstream and downstream boundaries of a road segment can be prescribed in demand and supply respectively.

finally in the third step, we obtain the traffic density at the next time-step based on the conservation of traffic flow as

$$k_i' = k_i + \frac{\Delta t}{\Delta x}(\Phi_i - \Phi_{i+1}), \tag{6}$$

where Δt is the time-step size and Δx the cell length. Cell length Δx and time-step size Δt need to be chosen so as to respect the Courant Friedrich Lewy condition (Courant et al., 1967 [orig.: 1928]) such that $\Delta x/\Delta t > v_f$. Choosing an appropriate Δx thus depends indirectly on choosing a reasonable value for Δt and vice-versa.

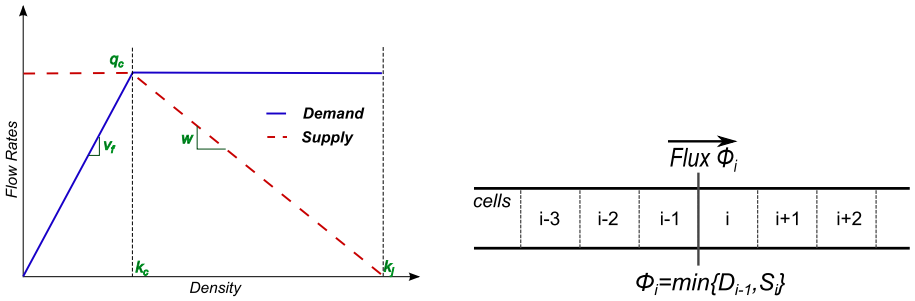

(a) Demand and Supply (b) Boundary flux

Figure 1: An illustration of the Cell Transmission Model

2.2. Queue discharge features in CTM

For a through movement, we assume that the traffic light turns green at $t = 0$ and the stop-line is at $x = 0$. In a queue discharge scenario, the initial traffic density is:

$$k(x, 0) = \begin{cases} k_j, & x < 0 \\ 0, & x > 0 \end{cases} \tag{7}$$

If in CTM we let the queue discharge process immediately start at $t = 0$, then the upstream demand and the downstream supply at $x = 0$ are always q_c, and the discharge flow-rate equals the saturation flow-rate; i.e., $q(0, t) = q_c$ for $t > 0$ till the queue disappears or the traffic light turns red. Correspondingly the queue discharge headway is the saturation headway $h = h_s = 1/q_c$. The solutions are shown in Figure 2a and Figure 2b. Such a model would clearly over-estimate the intersection capacity as the product of green time and capacity flow-rate (Dion et al., 2004) and may lead to suboptimal intersection design.

To accommodate the capacity lost due to start-up acceleration of vehicles, we can introduce a start-up lost time (Webster, 1958) in CTM. Traditionally, the start-up lost time is measured as total time difference between actual observed headways of vehicles and the saturation headway. We denote it by L_1. Thus the discharge flow-rate in CTM becomes

$$q(0, t) = \begin{cases} 0, & t < L_1 \\ q_c, & t \geq L_1 \end{cases} \tag{8}$$

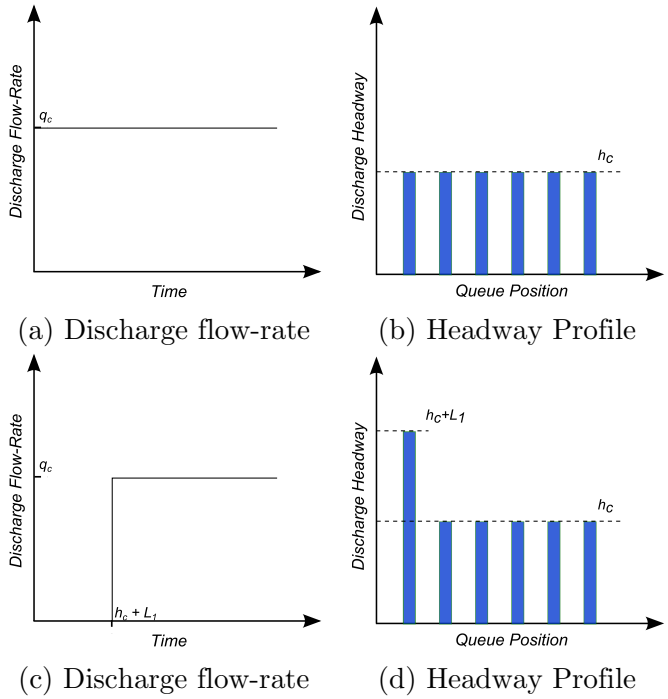

(a) Discharge flow-rate (b) Headway Profile

(c) Discharge flow-rate (d) Headway Profile

Figure 2: Discharge flow-rate and headway profiles in the traditional CTM: (2a, 2b) without lost time; (2c, 2d) with start-up lost time.

Correspondingly the first vehicle's lost time is increased by L_1. These solutions are shown in Figure 2c and Figure 2d. This model is more realistic, but even if the start-up lost time is accurate, it is not clear whether the cumulative flow is accurate. In addition, the discharge headways still do not match the observed pattern, and the corresponding dynamics are not correct.

3. A modified Cell Transmission Model

3.1. A new demand function and the modified CTM

In (Lebacque, 1984), where a network traffic simulation model was developed based on a Godunov discretization of the LWR model, it was argued that the queue discharge flow-rate should gradually increase from 0 to the saturation flow-rate after the traffic light turns green. But the implementation of this discharge feature was not discussed.

In this study, we modify CTM by applying a new demand function, which was introduced in (Lebacque, 2003) for a bounded acceleration extension of the LWR model. In the demand function, traffic demand in congested traffic is less than capacity and decreases with density. Note that the congested part of the demand function can be convex or concave in (Lebacque, 2003). (Monamy et al., 2012) applied the idea of a modified demand function at a node to capture the recovery flow under congested conditions. The demand used in the study is

dependent on the number of vehicles currently 'stored' in the node. The resultant was an overall reduced recovery demand that was able to model features similar to observed capacity drop at test locations. Here we simply use a demand function that is linearly decreasing in density for congested traffic. That is,

$$D'(k) = \min\{v_f k,\ q_j + c^*(k_j - k)\} = \min\{v_f k,\ c^*(k_j^* - k)\}. \tag{9}$$

Figure 3 shows the new demand function along with definitions of parameters. In addition to the free-flow speed, jam density, and critical density, which are used in the definition of the traditional demand function, a new variable, called jam demand, q_j, is introduced as the demand at the jam density.

From the definitions of the variables, the following relations follow immediately:

$$q_c = c^*(k_j^* - k_c) = w(k_j - k_c), \tag{10}$$
$$q_j = c^*(k_j^* - k_j). \tag{11}$$

The slope of the demand curve c^* (not to be confused with shock wave speed), and the extrapolated jam density for demand k_j^* can be derived from the four basic parameters and are also shown in the figure.

Therefore, the modified CTM is only different from the traditional CTM in the definition of the demand in congested traffic and has an additional parameter, the jam demand, but the definition of supply, the flux function, and the density updating equation are still the same as those in (4)-(6).

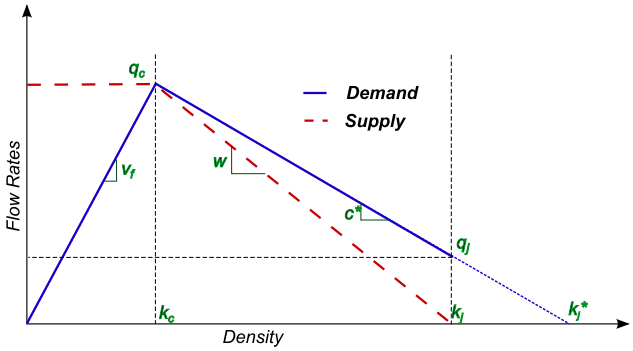

(a) Demand-Supply

v_f	*Free Flow Speed*
q_c	*Capacity Flow Rate*
k_c	*Critical Density*
k_j	*Jam Density*
k_j^*	*Projected Jam Density for Demand*
q_j	*Jam Demand Flow Rate*
w	*Slope of Supply Curve when k > kc*
c^*	*Slope of Demand Curve when k > kc*

(b) Variables

Figure 3: The modified demand function along with list of variable definitions

3.2. Solutions to the Riemann problem

The new demand function and, therefore, the modified CTM are primarily proposed to obtain more realistic solutions under the queue discharge initial condition in (7). In this

subsection, however, we demonstrate that the new model is also well defined under more general Riemann initial conditions:

$$k(x,0) = \begin{cases} k_u, & x < 0 \\ k_d, & x > 0 \end{cases} \tag{12}$$

where k_u is the upstream density and k_d the downstream density. The corresponding initial flow-rates are denoted by $q_u = Q(k_u)$ and $q_d = Q(k_d)$.

Following (Lebacque, 1996), we will consider the numerical solutions to the modified CTM in the seven scenarios, where traffic is (strictly) under-critical if density is (strictly) lower than the critical density, and (strictly) over-critical if density is (strictly) higher than the critical density.

Note that the new demand function is different from the traditional function only when $k > k_c$. Thus the solutions to the Riemann problem are the same for most of the cases, and here we only focus on the scenarios when the modified CTM has different solutions with possible additional sub-scenarios. The seven resulting scenarios are:

- Case I, II: Both upstream and downstream under-critical: $k_u > k_d$ or $k_u \leq k_d$. Since the new demand function is the same as the traditional one in these cases, the solutions to the Riemann problem remain the same with the modified CTM: there arises a rarefaction wave in Case I and a shock wave in Case II.

- Case III, IV: Upstream under-critical, downstream over-critical, $q_u < q_d$ or $q_u \geq q_d$. Similar to cases I and II, these cases lead to the same solutions between the modified and traditional CTM: there arises a shock wave with a positive speed in Case III and a shock wave with a negative speed in Case IV.

- Case V: Upstream over-critical, downstream over-critical, $k_u > k_d$. When the upstream density is higher, in the traditional model, a rarefaction wave arises along with accelerating vehicles, and the discharging flow-rate $q(0,t) = S(k_d)$ since $D(k_u) = q_c > S(k_d)$. But in the modified CTM, since $D'(k_u)$ can be smaller than $S(k_d)$, we further separate this case into two sub-cases.

  - Case V-a: $D'(k_u) \geq S(k_d)$. In this case the solutions are the same for the modified and traditional CTM.
  - Case V-b: $D'(k_u) < S(k_d)$. This condition is same as

$$k_c < k_d < k_c + \frac{w^*}{w}(k_u - k_c). \tag{13}$$

    As an example, the solutions to the traditional and modified CTM are shown in Figure 4, where $v_f = 35.19$, $q_c = 1900$, $w = 12.18$, $q_j = 750$, $k_u = 80$ vpm, and $k_d = 60$ vpm. Clearly (13) is satisfied. We can see that, in the modified CTM, the solutions show a discharge like behavior: The initial speed of a discharging

vehicle is lower than the speed of downstream block of vehicles. This creates a 'vacuum' condition (zero density) between the first discharged vehicle and the downstream platoon. This region increases in length as the discharged vehicle accelerates up to the downstream platoon's speed. The discharged vehicle is able to accelerate beyond the speed of the downstream platoon due to this 'vacuum' area and eventually catches up with the downstream block creating a shockwave.

- Case VI: Upstream over-critical, downstream over-critical, $k_u \leq k_d$. In this case, the upstream demand is always higher than the downstream supply, and the discharging flow-rate is controlled by the downstream supply. Thus in this case the solution is once again unchanged from the traditional model.

- Case VII: Upstream strictly over-critical, downstream strictly under-critical. This case is a more generalized form of the queue discharge scenario in (7), and vehicles discharge from congested platoons to an unrestrictive downstream link. The qualitative results of such a case are discussed in Section 4 (see Figure 6) and further from data validation results in Figure 10. The upstream demand stays in the modified over-critical region, while the downstream supply stays at capacity. The scenario results in formation of rarefaction waves as shown in Figure 5.

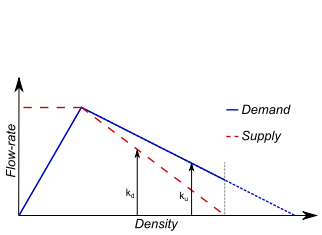

(a) Initial densities

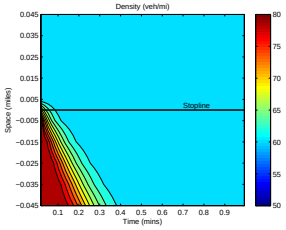

(b) Trad. CTM densities

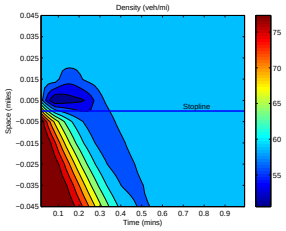

(c) Mod. CTM densities

Capacity	1900 veh/hr
Critical Density	54 veh/mi
Jam Density	210 veh/mi
Jam Demand	750 veh/hr
Cell Length	0.01 mi
Initial k_u	80 veh/mi
Initial k_d	60 veh/mi

(d) Parameter values

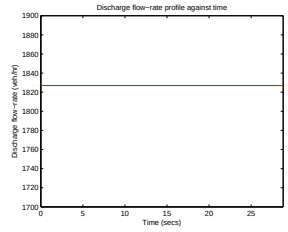

(e) Trad. CTM flow-rate

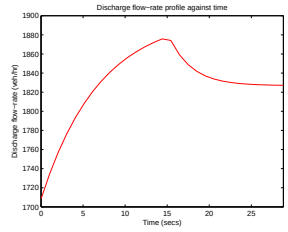

(f) Mod. CTM flow-rate

Figure 4: Comparison of density contour plots between the traditional and modified CTM in Case V-b.

4. Queue discharge features of the modified CTM

In this section, we analytically solve the modified CTM for the queue discharge scenario under the initial condition given in (7). From the solutions we will reveal queue discharge

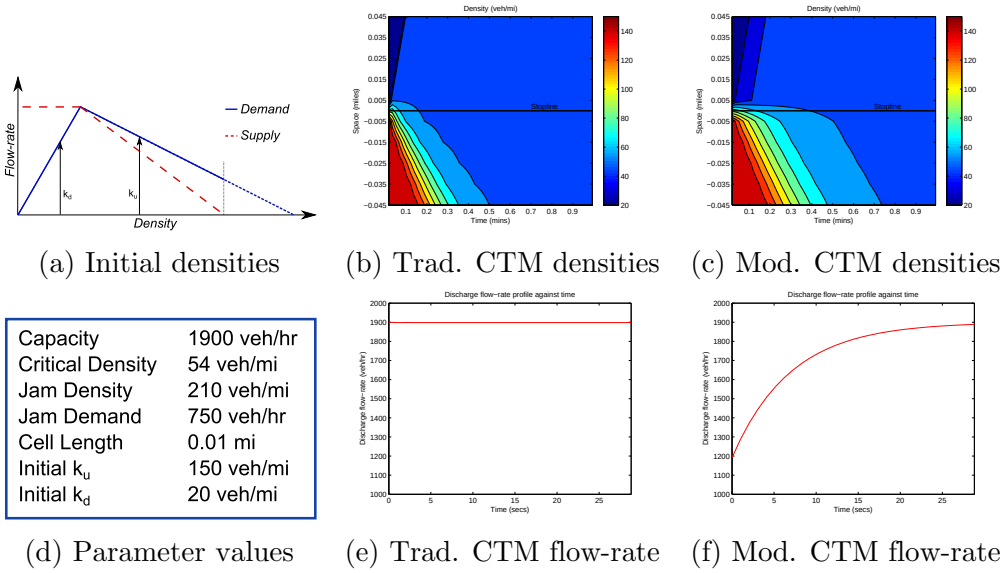

(a) Initial densities (b) Trad. CTM densities (c) Mod. CTM densities

(d) Parameter values (e) Trad. CTM flow-rate (f) Mod. CTM flow-rate

Figure 5: Comparison of density contour plots between the traditional and modified CTM in case VII.

features of the new model.

4.1. Discharge flow-rate and headway

We denote the density of the cell upstream to the stop-line by $k(t)$, and the cell length by L. For the queue discharge scenario, cells upstream to the stop-line are always over-critical, and those downstream always under-critical. Thus the in-flux of the studied cell is determined by its supply, $w(k_j - k)$, and its out-flux by its demand, $c^*(k_j^* - k)$. For the purpose of simple analysis, we approximate the discrete CTM, (6), by the following ordinary differential equation:

$$L\frac{dk}{dt} = w(k_j - k) - c^*(k_j^* - k), \tag{14}$$

where the initial condition is $k(0) = k_j$. In addition, the queue discharge flow-rate is given by the out-flux

$$q(0,t) = c^*(k_j^* - k). \tag{15}$$

From (10), we can simplify the right-hand side of (14) as $(w - c^*)(k_c - k)$. Thus solving (14), we obtain the time-dependent density in the cell upstream to the stop-line as:

$$k(t) = (k_j - k_c)e^{\frac{c^* - w}{L}t} + k_c, \tag{16}$$

which decreases in time since $c^* < w$ and converges to k_c asymptotically. Correspondingly the discharge flow-rate is given by:

$$q(0,t) = q_c - c^*(k_j - k_c)e^{\frac{c^* - w}{L}t}, \tag{17}$$

which increases from $q_j = c^*(k_j^* - k_j)$ at $t = 0$ to q_c asymptotically. Thus the jam demand, q_j, is also the initial discharge flow-rate. The resulting discharge flow-rate has the same exponential form as that estimated from observations in (Akçelik et al., 1999; Akçelik and Besley, 2002).

We denote the cumulative number of vehicles passing the stop-line by $A(t)$ and obtain from (17)

$$A(t) \;=\; \int_{s=0}^{t} q(0,s)ds = q_c t + \frac{L}{c^* - w} c^*(k_j - k_c)(1 - e^{\frac{c^* - w}{L} t}), \tag{18}$$

which is an increasing function in time t. Then the passing time is the inverse function

$$T(a) \;=\; A^{-1}(a), \tag{19}$$

and the time for vehicle n to pass the stop-line is t_n:

$$t_n \;=\; T(n). \tag{20}$$

We denote the continuous headway by $h(t)$. Then

$$h(t) \;=\; \frac{1}{q(0,t)} = \frac{1}{q_c - c^*(k_j - k_c)e^{\frac{c^* - w}{L} t}}, \tag{21}$$

which decreases from $\frac{1}{q_j}$ to the saturation headway $h_s = \frac{1}{q_c}$. If we denote the discrete headway of vehicle n by h_n, then after solving t_n from (20) we have ($n = 1, 2, \cdots$)

$$h_n \;=\; t_n - t_{n-1}, \tag{22}$$

where we let $t_0 = 0$. From (20) and (22) we have

$$q_c h_n + \frac{c^*}{c^* - w}(k_j - k_c) L e^{\frac{c^* - w}{L} t_{n-1}} (e^{h_n} - 1) \;=\; 1. \tag{23}$$

Since $t_{n-1} \to \infty$, we can see that the discrete headway also converges to the saturation headway; i.e., $h_n \to h_s = \frac{1}{q_c}$.

In Figure 6, we demonstrate the demand and supply functions in Figure 6a, the discharge flow-rate in Figure 6b, the continuous headway in Figure 6c, and the discrete headways in Figure 6d.

4.2. Lost Times

During the queue discharge process, the start-up lost time, L_1, is defined as the sum of the differences between all headways and the saturation headway (Roess et al., 2010):

$$L_1 \;=\; \sum_{n=1}^{\infty} (h_n - h_s). \tag{24}$$

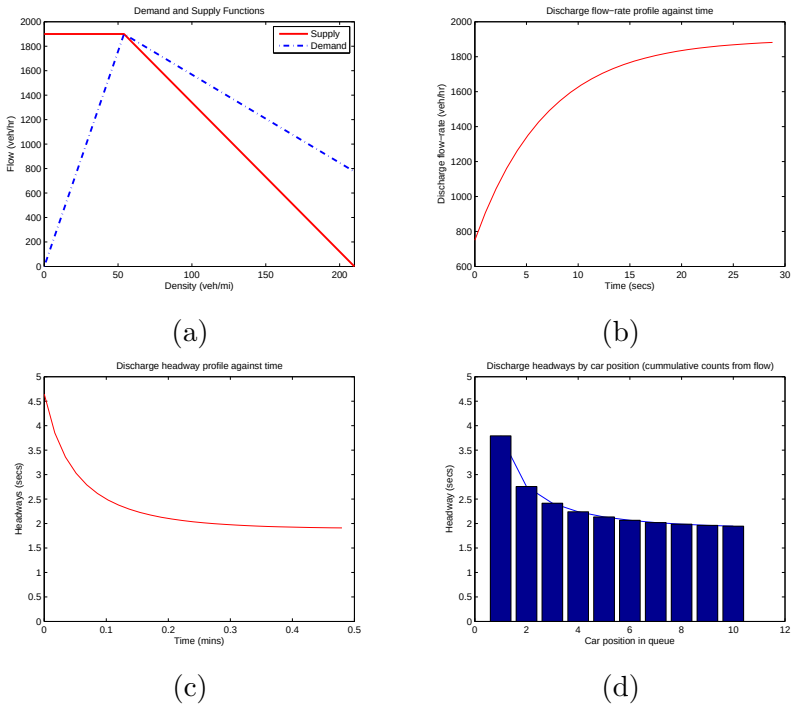

Figure 6: Queue discharge flow-rate and headways: (a) demand and supply curves; (b) discharge flow-rate; (c) continuous headways; and (d) discrete headways. The results shown are for $q_c = 1900$, $k_c = 54$, $k_j = 210$, and $q_j = 775$, with upstream fully congested at jam density, and downstream density set to 0 as initial conditions.

From (22) and (18), we can see that

$$L_1 \quad = \quad \lim_{a\to\infty} T(a) - h_s a = \lim_{t\to\infty} t - \frac{A(t)}{q_c} = \frac{L}{w - c^*}\frac{c^*}{w}. \tag{25}$$

Furthermore, from (18) we can see that $\lim_{t\to\infty} A(t) = q_c(t - L_1)$. That is, $q_c(t - L_1)$ is the asymptotic line of $A(t)$. Compared with the ideal situation when the discharge flow-rate is always q_c, there is a lost capacity (as shown in Figure 7) of:

$$\Delta C \quad = \quad \lim_{t\to\infty} q_c t - A(t) = q_c L_1. \tag{26}$$

This justifies the idea of the effective green time in (8); that is, if the start-up lost time L_1 is defined as in (25), then the total number of discharged vehicles will be equivalent if we use the new CTM model or (8).

5. Calibration and validation

The presented model can be calibrated using minimal additional headway observations if the macroscopic variables associated with traffic behavior at the intersection are known (note

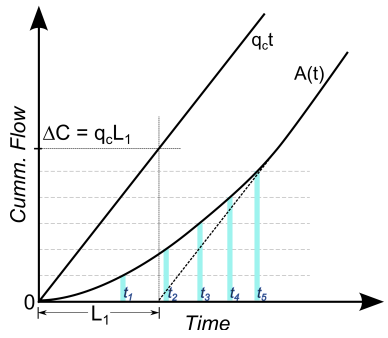

Figure 7: Relation between lost capacity and start-up lost time. The figure illustrates how the cumulative flow from the modified model, $A(t)$, is asymptotic to the line $q_c(t - L_1)$. The figure also shows the corresponding passing time of each queued vehicle t_i.

that if an appropriate value for L is known, q_j and c^* can be calibrated directly knowing either the headway of the first vehicle, or the total lost time (25)). However, for robust calibration, detailed headway observations are recommended. Where vehicle headway observations are available, statistical fitting techniques can be used to calibrate the parameters of the model. This is in fact the approach we take in the current study.

5.1. Approach

In the traditional CTM, we need to calibrate the three parameters in the triangular fundamental diagram (2), and the demand and supply functions in (3)-(4): the capacity flow-rate (saturation flow-rate), q_c, the critical density, k_c, and the jam density of queued vehicles, k_j; then v_f and w can be calculated as $v_f = q_c/k_c$ and $w = q_c/(k_j - k_c)$.

For the modified CTM, we need to calibrate an additional parameter for the modified demand function in (9): the jam demand, q_j. From observations of discharge headways at an intersection, the corresponding passing times for vehicles as they cross the stop-line, t_i, can be obtained. From the modified CTM, we also know the cumulative number of vehicles passing the stop-line as a function of time and the parameters w, c^*, k_c, q_c, k_j and L (18). However, the relation can be re-written using the unique parameter set: k_c, q_c, k_j, q_j, and L, using (10)-(11). We use the notation $\hat{A}(t)$ here to highlight that this is the modeled prediction in the optimization setup:

$$\hat{A}(t) \;=\; q_c t - L\left(\frac{q_c - q_j}{q_j}\right)(k_j - k_c)\left(1 - e^{-\frac{q_j}{L(k_j - k_c)}t}\right). \tag{27}$$

We can then obtain the predicted cumulative count of vehicles corresponding to actual observed passing times of each vehicle. Thus, an optimization problem can be set up on the cumulative vehicle counts (with passing time as the independent variable) (Figure 8). We use minimization of the Sum of Squared Errors as the optimization criterion here.

$$\begin{aligned} \underset{X}{\text{minimize}} \quad & \sum_{i=1}^{n} \left(\hat{A}(X, t_i) - i \right)^2, \\ \text{where,} \quad & X = \{k_c, q_c, k_j, q_j, L\}, \\ \text{subject to:} \quad & X_L \leq X \leq X_H. \end{aligned} \tag{28}$$

Discharge headway data is only applicable for those vehicles that are part of the standing queue before the discharge process starts. This means that the number of data points in the optimization is restricted by the length of the standing queue observed at the location of interest (typically 5-10 vehicles). Since the model requires the calibration of five parameters, thus having a high degree of freedom, there is an inherent risk of over-fitting unless constraints are imposed on the parameters. It is thus imperative to ensure that certain ranges are imposed on the values of the calibration parameters, or that some of the parameters are held constant based on knowledge of traffic behavior at the location (forming the constraints in the optimization setup).

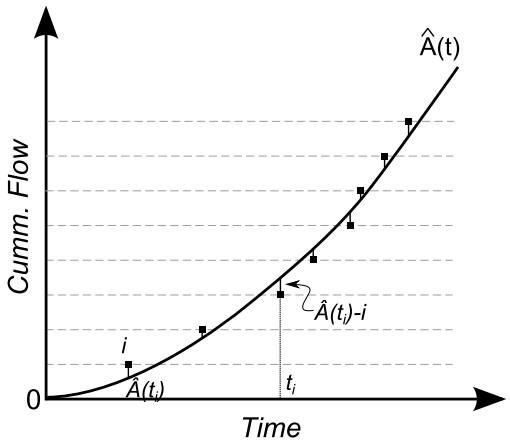

Figure 8: The figure illustrates the setup of the calibration process. $\hat{A}(t)$ is the predicted cumulative flow at time t from the model, while the observed passing times for vehicle i are shown as t_i. Since $\hat{A}(t_i)$ represents the modeled cumulative flow corresponding to the observed passing time of the i^{th} vehicle, the objective of the optimization is to minimize $\sum(\hat{A}(t_i) - i)^2$

5.2. Calibration

As part of the present study, the linear demand model was calibrated for three data sets: data from various headway studies in past literature, NGSIM (FHWA, 2007) data from Lankershim Blvd., and video recordings from a local study site. Calibration of the model was done for each location individually and employed knowledge of certain features such as free-flow speed and jam density where available.

The first data set used for the calibration process, was obtained from headway studies from past literature. (Gerlough and Wagner, 1967), (Hung et al., 2002), and Tong and

Hung's simulation results (Tong and Hung, 2002) have presented various study results on headway data. The model was calibrated for each of the three sets of headway observations.

NGSIM data of through moving traffic from Lankershim Blvd SB, at its intersection with Universal Hollywood Dr (Figure 9b) was used as the second data set. The study site offers clear camera visibility and supports a steady demand for through movements. The location has 3 through lanes (1 shared right turn lane). Only vehicles in a standing queue at start of green phase were recorded. Observations suggested a critical density of 54 veh/mi, jam density of 210 veh/mi, and a saturated headway of roughly 1.8 sec at the location.

(a) E. Peltason Dr (Recording)

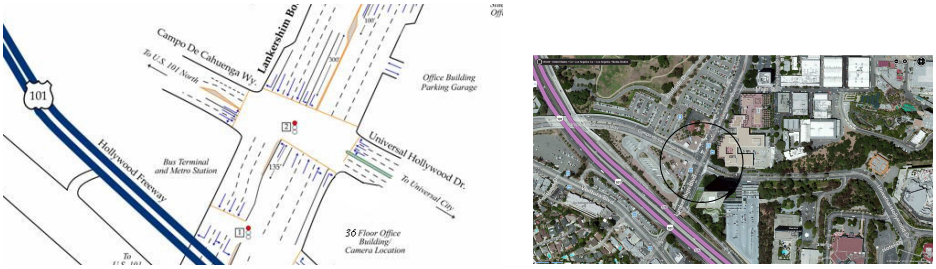

(b) Lankershim Blvd (NGSIM)

Figure 9: Schematic Diagrams and aerial maps of the two study sites: 9a. E. Peltason Dr. in Irvine, CA; and 9b. Lankershim Blvd. and Universal Hollywood Dr. in Los Angeles, CA (Maps coutesy Bing)

Finally, a video recording study site was chosen for additional data collection near the University of California, Irvine campus, at a push button pedestrian crossing signal on E. Peltason (between Los Trancos Drive, and Anteater Drive; shown in Figure 9a). The location offered observations of single-lane traffic at an intersection that allowed only through movements. Using a video recording device, the headways of vehicles (by queue positions) were observed over multiple cycles and averaged to obtain the headways vs. queue position curve. Still photographs of queued vehicles at the location suggested the jam density to be in the range of 210 veh/mi. The free-flow speed at the location was observed to be 35 mi/hr (30 mi/hr posted speed limit).

The observation of the critical density from the data was used to fix the k_c value for all 5 experiments as a value of 54veh/mi. Similarly, L was held constant at 0.01 mi. The jam density k_j was also set to 210 veh/mi for 4 out of 5 experiments (the exception being data from Gerlough and Wagner's study where k_j was also an optimization variable). The calibration technique used was the minimization problem in (28). MATLAB's implementation

of the Nelder-Mead heuristic search (Nelder and Mead, 1965) was used to find the solution to the non-linear optimization, and the results were verified against Generalized Reduced Gradient technique.

The final form of the optimization problem for the datasets used was:

$$\begin{aligned} \underset{\{k_c,q_c,k_j,q_j,L\}}{\text{minimize}} \quad & \sum_{i=1}^{n} \left(q_c t - L \left(\frac{q_c - q_j}{q_j} \right) (k_j - k_c) \left(1 - e^{-\frac{q_j}{L(k_j - k_c)} t} \right) - i \right)^2, \\ \text{subject to:} \quad & k_c = 54, \\ & 1200 \leq q_c \leq 2400, \\ & 80 \leq k_j \leq 280, \\ & k_j = 210, \text{(for all cases excluding Gerlough and Wagner)}, \\ & 0 \leq q_j \leq 1500, \\ & L = 0.01. \end{aligned} \tag{29}$$

Table 1 presents results from the calibration process. The reported sum of squared errors (SSE) and R^2 values in the table were calculated for headways and not the inverse function that the fitting was performed on. The SSE, thus, is the sum of squared differences between the model-predicted headway and the actual observed headway for each queue position. Similarly, R^2 was calculated as $1-(SSE/SS_{tot})$ where SS_{tot} is the sum of squared differences of observed headway with mean headway (proportional to variance of observed data). Figure 10 shows the calibrated demand supply functions and the derived discharge headways as compared against observations for each of the cases. The calibration results suggest that the modified CTM indeed replicates realistic features of queue discharge to high accuracy. Note that, compared with those in (Gerlough and Wagner, 1967) and (Hung et al., 2002), the headway distributions show a higher variance in the tail due to the limited numbers of cycles for the NGSIM and Peltason data.

		Gerlough (1967)	Hung et. al. (2002)	Tong, Hung (2002)	NGSIM	Recordings
Capacity	(v/h/l)	1530	1760	1775	1950	1900
Critical Density	(v/m/l)	54	54	54	54	54
Jam Density	(v/m/l)	147	210	210	210	210
Jam Demand	(v/h/l)	730	733	630	775	750
L	(mi)	0.01	0.01	0.01	0.01	0.01
R^2		0.99	0.99	0.98	0.96	0.91
SSE	(sec^2)	0.04	0.02	0.07	0.14	0.45

Table 1: Headway fitting - Calibrated parameters for the various data sources along with the SSE obtained for each case.

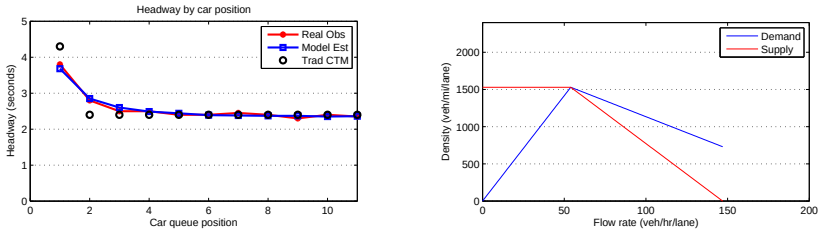

(a) Gerlough and Wagner (1967)

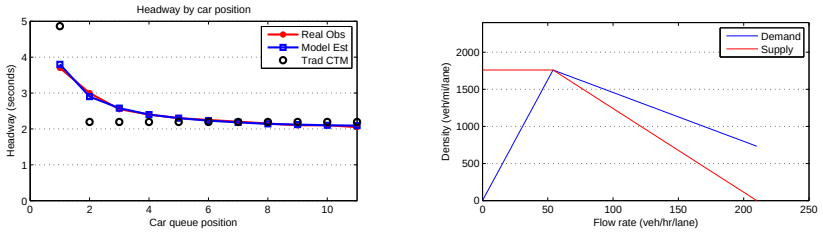

(b) Hung et. al. (2002)

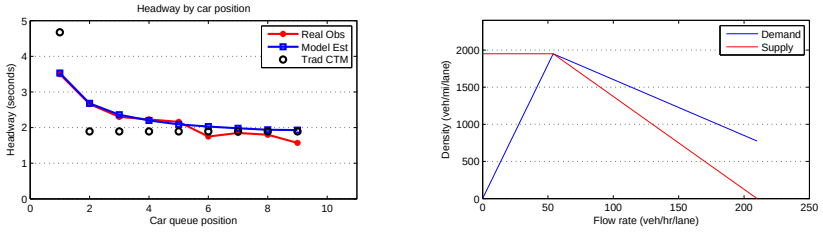

(c) NGSIM

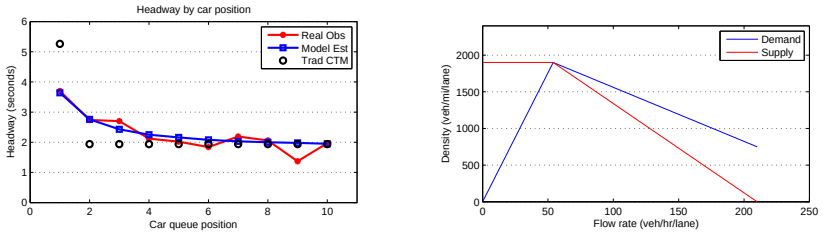

(d) E. Peltason (Video Recording)

Figure 10: Headway calibration for the various data sources showing the fitted headway curves and the corresponding demand-supply functions. The graphs depicting headways provides a comparison between observed headways, headways predicted by traditional CTM with lost time, and headways predicted by a calibrated modified CTM.

6. Conclusions

Signalized intersection capacity is typically estimated through calibration of lost times of vehicles discharging from a queue at the intersection. This lost time in turn is calculated from the differences between the headways observed by the leading vehicles and the saturation headway. The increased headway for the first few vehicles in the queue is attributed to the reaction times of drivers, as well as the bounded acceleration process involved. In order to

adjust for the lost discharge capacity during the initial seconds of the green phase due to higher headways, typically an assumption is made that puts the discharge capacity at zero for an initial period, followed by saturated capacity discharge.

In this paper, we proposed the use of a modified Cell Transmission Model with a new demand function, in order to capture realistic queue discharge features at an intersection when vehicles are accelerating away from an initial standing queue. The new model suggests that the demand immediately upstream of the discharge location is indeed not equal to the capacity, due to the vehicles' acceleration being bounded. Through the modeling of the reduced demand, the model is able to also capture the dynamics of traffic behavior at intersections. Further, the modification introduces a single additional parameter thus keeping the calibration process simple. The possibility of obtaining analytical results, as well as the computational tractability offers the model distinct advantages over more complex models.

We first show analytically that the resulting headway and discharge flow-rate profiles over time obtained through this queue discharge model are good representations of the expected shapes of those curves qualitatively. The model is then calibrated for data sets obtained from past headway studies as well as newly obtained data, and is shown to model the headways with good accuracy. A discussion on the similarities and comparisons of the existing 'Lost Time' based model and the currently proposed model reveals strengths of both the models. This discussion further leads to a more rigorous definition of the macroscopic 'lost time' and a means of estimating it from the model itself.

An interesting property of the modified CTM lies in the importance of choosing a reasonable time-step size Δt (or cell length L which is also constrained by Δt). The time-step size in the model is loosely related to the reaction time and the acceleration rates of the vehicles. A very small Δt would imply near-instantaneous reactions from drivers and vehicles, and thus result in a flattening of the headway curve with all discharging vehicles having identical headways. Conversely, a large Δt would imply that the initial vehicle would have a very large headway. Studying the model under various scenarios suggests that Δt should be chosen to be in the order of 1-2 seconds.

Queue discharge dynamics and the effects of bounded acceleration can also be captured through higher-order models and hybrid models. Bounded acceleration extensions to the CTM framework (Lebacque, 1997, 2003; Leclercq, 2002) can also be used to catch the behavior of vehicles accelerating from a queue at intersections to produce similar results. However, such models do not lend themselves easily to mathematical analysis, and typically require higher degrees of calibration efforts. To the best of our knowledge, there have not been any calibration and validation studies that compare performances of such models against observed data at arterial intersections, which highlights their complex structure. It would be an interesting extension to compare the performance of such higher order models against the currently proposed model calibrated from observed data. Similarly, though the piecewise linear demand function is a reasonable approximation of the effect of acceleration of vehicles, exploration of other shapes of the demand function could be an interesting study.

This study opens up a debate on macroscopic modeling of intersections that can capture

the lost capacity phenomenon at signals due to bounded accelerations and reaction times. Among the many possible extensions of this model, addition of an intersection model could offer a framework for analyzing the effects of the lost capacity over more complex networks of arterial roadways and intersections. Another possible extension could be exploring the portability of the calibrated parameters between locations, as well as studying how factors such as driver aggression and control measures affect the various parameters of the model. The proposed model is able to offer insights into such aspects as the capacity of the network, and prospectively through further extensions, observations such as capacity reductions in network fundamental diagrams and impacts of autonomous vehicles.

Acknowledgments

The research by the first two authors is partially supported by the University of California Transportation Center through a faculty grant.

References

Akçelik, R., Besley, M., 2002. Queue discharge flow and speed models for signalised intersections. In: Transportation and Traffic Theory in the 21st Century, Proceedings of the 15th International Symposium on Transportation and Traffic Theory. pp. 99--118.

Akçelik, R., Besley, M., Roper, R., 1999. Funaamental relationships for traffic flows at signalised intersections. Research Report ARR 340. ARRB Transport Research Ltd., Vermont South, Australia.

Al-Ghamdi, A. S., 1999. Entering headway for through movements at urban signalized intersections. Transportation Research Record: Journal of the Transportation Research Board 1678, 42--47.

Bloomberg, L., Dale, J., 2000. Comparison of vissim and corsim traffic simulation models on a congested network. Transportation Research Record: Journal of the Transportation Research Board 1727, 52--60.

Chen, L., Jin, W.-L., Hu, J., Zhang, Y., 2008. An urban intersection model based on multi-commodity kinematic wave theories. In: Proceedings of the 11th International IEEE Conference on Intelligent Transportation Systems. IEEE, pp. 269--274.

Courant, R., Friedrichs, K., Lewy, H., 1967 [orig.: 1928]. On the partial difference equations of mathematical physics. IBM journal of Research and Development 11 (2), 215--234.

Daganzo, C. F., 1995. The cell transmission model, part ii: network traffic. Transportation Research Part B 29 (2), 79--93.

Dion, F., Rakha, H., Kang, Y.-S., 2004. Comparison of delay estimates at under-saturated and over-saturated pre-timed signalized intersections. Transportation Research Part B 38 (2), 99--122.

FHWA, 2007. Ngsim - next generation simulation. Tech. rep.
URL `http://www.ngsim.fhwa.dot.gov`

Gerlough, D. L., Wagner, F. A., 1967. Improved criteria for traffic signals at individual intersections. Tech. rep., Transportation Research Board.

Geroliminis, N., Skabardonis, A., 2005. Prediction of arrival profiles and queue lengths along signalized arterials by using a markov decision process. Transportation Research Record: Journal of the Transportation Research Board 1934, 116--124.

Greenshields, B. D., Schapiro, D., Ericksen, E. L., 1946. Traffic performance at urban street intersections. Tech. rep.

Hung, W., Tian, F., Tong, H., 2002. Departure headways at one signalized junction in hong kong. In: Proceedings of Better Air Quality: Tales of Pacific Rim Megacities Workshop, Hong Kong.

Jin, W.-L., Gan, Q.-J., Gayah, V. V., 2013. A kinematic wave approach to traffic statics and dynamics in a double-ring network. Transportation Research Part B 57, 114--131.

King, G. F., Wilkinson, M., 1977. Relationship of signal design to discharge headway, approach capacity, and delay. Transportation Research Record (615), 37--44.

Kunzman, W., 1978. Another look at signalized intersection capacity. ITE journal 48 (HS-024 726), 12--15.

Lebacque, J.-P., 1984. Semi-macroscopic simulation of urban traffic. Proceedings of the International ASME Conference Modeling and Simulation 4, 273--292.

Lebacque, J.-P., 1993. Les modeles macroscopiques de trafic. In: Annales des Ponts et chaussées. No. 67. Elsevier, pp. 24--45.

Lebacque, J.-P., 1996. The godunov scheme and what it means for first order traffic flow models. In: Internaional symposium on transportation and traffic theory. pp. 647--677.

Lebacque, J.-P., 1997. A finite acceleration scheme for first order macroscopic traffic flow models. The 8th IFAC Symposium.

Lebacque, J.-P., 2003. Two-phase bounded-acceleration traffic flow model: analytical solutions and applications. Transportation Research Record: Journal of the Transportation Research Board 1852, 220--230.

Leclercq, L., 2002. Modélisation dynamique du trafic et applications à l'estimation du bruit routier. Ph.D. thesis, Villeurbanne, INSA.

Lee, J. J., Chen, R., 1986. Entering headway at signalized intersections in a small metropolitan area. Transportation Research Record (1091), 117--126.

Li, L., Wang, F.-Y., 2006. Approximate vehicle waiting time estimation using adaptive video-based vehicle tracking. In: Advances in Machine Vision, Image Processing, and Pattern Analysis. Springer, pp. 105--114.

Lighthill, M. J., Whitham, G. B., 1955. On kinematic waves. ii. a theory of traffic flow on long crowded roads. Proceedings of the Royal Society of London. Series A. Mathematical and Physical Sciences 229 (1178), 317--345.

Lo, H., 1999. A dynamic traffic assignment formulation that encapsulates the cell-transmission model. In: 14th International Symposium on Transportation and Traffic Theory.

Michalopoulos, P. G., Stephanopoulos, G., Stephanopoulos, G., 1981. An application of shock wave theory to traffic signal control. Transportation Research Part B 15 (1), 35--51.

Monamy, T., Haj-Salem, H., Lebacque, J.-P., 2012. A macroscopic node model related to capacity drop. Procedia-Social and Behavioral Sciences 54, 1388--1396.

Moussavi, M., Tarawneh, M., 1990. Variability of departure headways at signalized intersections. ITE 1990 Compendium of Technical Papers, 313--317.

Nelder, J. A., Mead, R., 1965. A simplex method for function minimization. The computer journal 7 (4), 308--313.

Niittymäki, J., Pursula, M., 1997. Saturation flows at signal-group-controlled traffic signals. Transportation Research Record: Journal of the Transportation Research Board 1572 (1), 24--32.

Pacey, G., 1956. The progress of a bunch of vehicles released from a traffic signal. Road Research Laboratory Note RN/2665/GMP.

Richards, P. I., 1956. Shock waves on the highway. Operations research 4 (1), 42--51.

Robertson, D. I., 1969. Transyt: a traffic network study tool.

Roess, R., Prassas, E., McShane, W., 2010. Traffic engineering. Prentice Hall.

Stephanopoulos, G., Michalopoulos, P. G., Stephanopoulos, G., 1979. Modelling and analysis of traffic queue dynamics at signalized intersections. Transportation Research Part A 13 (5), 295--307.

Tian, Z. Z., Urbanik, T., Engelbrecht, R., Balke, K., 2002. Variations in capacity and delay estimates from microscopic traffic simulation models. Transportation Research Record: Journal of the Transportation Research Board 1802, 23--31.

Tong, H., Hung, W., 2002. Neural network modeling of vehicle discharge headway at signalized intersection: model descriptions and results. Transportation Research Part A 36 (1), 17--40.

Webster, F. V., 1958. Traffic signal settings. Tech. rep.